Asymptotically stable control for a nonlinear-based multirotor aerial vehicle model

Igor Afonso Acampora Prado[1,a], Davi Ferreira de Castro[1,b], and Mateus de Freitas Virgílio Pereira[1,c], Davi Antônio dos Santos[1,d] and José Manoel Balthazar[e]
[1]Instituto Tecnológico de Aeronáutica, ITA, Brazil.

Abstract. The interest for multirotor aerial vehicles (MAVs) is currently growing due to their low cost, high manoeuvrability, simplified mechanics, capability to perform vertical take-off and landing as well as hovering flight. These characteristics make them a promising technology suitable for applications such as suveillance of indoor and urban environments. The present work faces the problem of controlling the attitude of a MAV by means of a linear feedback control which guarantees asymptotic stability when controlling a nonlinear dynamics. The simulations show the effectiveness of the method.

1 Introduction

Multirotor Aerial Vehicles (MAVs) have motivated many researches in different fields of knowledge such as sensors fusion [3], computer vision [7] and control strategies [6]. Although there is a massive amount of concluded and ongoing research works on MAVs, the design of control laws for such vehicles still has challenges to be overcome. Most of those challenges are related to design control laws that guarantee asymptotic stability, mostly because this system is nonlinear.

Reference [2] presents two nonlinear control techniques, backstepping and sliding mode, in order to control the attitude of the MAV. On the other hand, reference [4] utilizes a nonlinear H_∞ controller to stabilize the rotational movements. Both strategies have a high degree of complexity. Therefore, it would be interesting to design a linear feedback control which also guarantees stability for a nonlinear system.

The Linear Quadratic Regulator (LQR) is an usual control strategy applied to MAVs [1], which requires a linear design model. Such linear model does not take into account the nonlinear phenomena that are present in the real operation of these vehicles. However, for a more effective control law, nonlinearities have to be considered in order to avoid unstable regions of operation. One of the nonlinearities included in the motion equations is the gyroscopic effects which come from the rotation of the rigid body and the four propellers.

This paper uses the [5] theorem to stabilize the attitude of a MAV. This theorem showed that is possible to construct a linear feedback control law for a nonlinear dynamics that is globally asymptotically stable.

[a] e-mail: igorap@ita.br
[b] e-mail: davifc@ita.br
[c] e-mail: mateusfvp@hotmail.com
[d] e-mail: davists@ita.br
[e] e-mail: jmbaltha@ita.br

2 MAV Modeling

This section presents the equations of motion of a multirotor aerial vehicle (MAV), considering all the relevant effects necessary to be accounted for in ground-thruth model for simulation-based evaluation of control laws. We start with preliminary definitions in Subsection 2.1, then we present the rotor dynamics in 2.2 and the MAV rotational dynamics in 2.3.

2.1 Preliminary definitions

We define two Cartesian coordinate systems (CCS) as illustrated in Figure 1. The body CCS, $S_B \triangleq \{X_B, Y_B, Z_B\}$ is attached to the vehicle's body with the origin at the vehicle's center of mass (CM), the X_B axis pointing forward, the Z_B axis pointing upward, perpendicular to the plane of the rotors, and the Y_B axis completing a dextrogeous frame. The CCS, $S_G = \{X_G, Y_G, Z_G\}$ is fixed to the ground at a known point O, with the Z_G axis pointing upward, aligned with the local vertical.

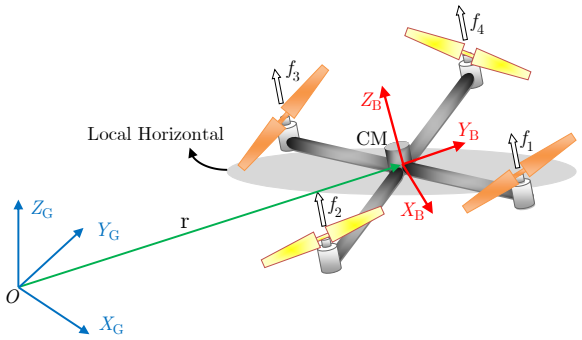

Fig. 1. The Cartesian coordinate systems (CCS). $S_B = \{X_B, Y_B, Z_B\}$ is the body CCS and $S_G = \{X_G, Y_G, Z_G\}$ is the ground CCS.

2.2 Rotor dynamics

The thrust force f_i and reaction torque τ_i produced by each individual rotor are modeled, respectively, by the aerodynamic models

$$f_i = k_f \omega_i^2, \tag{1}$$

$$\tau_i = k_\tau \omega_i^2, \tag{2}$$

for $i = 1, ..., 4$, where k_f is the force coefficient, k_τ is the torque coefficient, and ω_i is the rotation speed of the ith rotor (positive in courterclockwise direction), whose dynamics can be modeled by the following first-order linear model:

$$\dot{\omega}_i = -\frac{1}{\tau_\omega}\omega_i + \frac{k_\omega}{\tau_\omega}\bar{\omega}_i \tag{3}$$

where $\bar{\omega}_i \in [0, \bar{\omega}_{\max}]$ is the rotation speed command for the ith rotor, k_ω is the rotation coefficient, and τ_ω is rotor time constant.

2.3 Resultant control thrust and torque

Although the formulation given here could be generalized to any multirotor vehicle configuration, for illustration purpose, we consider a quadrotor configuration with the longitudinal axis X_B pointing between rotor 1 and rotor 2, and with 45 degree of separation angle between adjacent arms; we call it the "x" configuration. Moreover, we consider that rotor 1 and rotor 3 rotate in clockwise direction, while rotor 2 and rotor 4 rotate in counterclockwise direction. For the aforementioned configuration, one can show that the relationship between the individual rotor thrusts f_i and the resultant thrust magnitude and torque vector is given by

$$\begin{bmatrix} F^c \\ \mathbf{T}^c \end{bmatrix} = \boldsymbol{\Gamma}\mathbf{f}, \tag{4}$$

with $\mathbf{f} \triangleq \begin{bmatrix} f_1 & f_2 & f_3 & f_4 \end{bmatrix}^{\mathrm{T}}$ and

$$\boldsymbol{\Gamma} \triangleq \begin{bmatrix} 1 & 1 & 1 & 1 \\ l/\sqrt{2} & -l/\sqrt{2} & -l/\sqrt{2} & l/\sqrt{2} \\ -l/\sqrt{2} & -l/\sqrt{2} & l/\sqrt{2} & l/\sqrt{2} \\ k_\tau/k_f & -k_\tau/k_f & k_\tau/k_f & -k_\tau/k_f \end{bmatrix}, \tag{5}$$

where l is the length of each vehicle's arm. The superscript c in Eq. (5) stands for the control command defined by the operator and is used to distinguish from the other sources of force and torque that will be presented soon.

By inverting Eq. (5), one can compute the command $\bar{\mathbf{f}} \triangleq \begin{bmatrix} \bar{f}_1 & \bar{f}_2 & \bar{f}_3 & \bar{f}_4 \end{bmatrix}^{\mathrm{T}}$ as

$$\bar{\mathbf{f}} = \Xi \begin{bmatrix} \bar{F}^c \\ \bar{\mathbf{T}}^c \end{bmatrix}, \tag{6}$$

where $\Xi \triangleq \Gamma^{-1}$, $\bar{F}^c$ is the thrust magnitude command, and $\bar{\mathbf{T}}^c$ is the control torque command.

2.4 Rotational motion

Representing the attitude using the Euler angles $\boldsymbol{\alpha} \triangleq \begin{bmatrix} \phi & \theta & \psi \end{bmatrix}^{\mathrm{T}}$ in the rotation sequence 1-2-3, we have the following rotational kinematics equations:

$$\dot{\boldsymbol{\alpha}} = \mathcal{A}\boldsymbol{\Omega} \tag{7}$$

where $\boldsymbol{\Omega} \triangleq \begin{bmatrix} \Omega_x & \Omega_y & \Omega_z \end{bmatrix}^{\mathrm{T}}$ is the S_B representation of the vehicle's angular velocity w.r.t. S_G and

$$\mathcal{A} \triangleq \begin{bmatrix} \cos\psi/\cos\theta & -\sin\phi/\cos\theta & 0 \\ \sin\psi & \cos\psi & 0 \\ -\cos\psi\sin\theta/\cos\theta & \sin\psi\sin\theta/\cos\theta & 1 \end{bmatrix} \tag{8}$$

Assume that the vechile has a rigid structure and S_G is an inertial frame. Considering the existence of gyroscopic effects, due to the rotors, and disturbance torques, and using the Newton-Euler formulation, one can model the rotational dynamics of the MAV by

$$\dot{\boldsymbol{\Omega}} = \mathbf{J}^{-1}(\mathbf{J}\boldsymbol{\Omega}) \times \boldsymbol{\Omega} + I_r \mathbf{J}^{-1}\boldsymbol{\Omega} \times \mathbf{e}_3 \sum_{i=1}^{4} (-1)^i \omega_i + \mathbf{J}^{-1}\mathbf{T}^c + \mathbf{J}^{-1}\mathbf{T}^d \tag{9}$$

where $\mathbf{T}^c$ and $\mathbf{T}^d$ are the S_B representations of the resultant control torque and disturbance torque, respectively, $\mathbf{e}_3 \triangleq [0 \ 0 \ 1]^{\mathrm{T}}$, I_r is the moment of inertia of the rotors w.r.t. the rotation axis, and $\mathbf{J}$ is the body inertia matrix. Consider that the vehicle has a symmetric structure with known mass m and inertia matrix in S_B

$$\mathbf{J} = \begin{bmatrix} J_x & 0 & 0 \\ 0 & J_y & 0 \\ 0 & 0 & J_z \end{bmatrix}. \tag{10}$$

This paper makes use of the AR Drone 2 parameters in order to emulate a real plataform. The values can be seen in Table 1.

3 State-space models

This section presents the nonlinear state-space model for rotation (Section 2). This model will be adopted for designing control laws by using the Rafikov and Balthazar's theorem. Firstly, note that the dynamics in Eq. (7) and (9) can be formulated as

$$\dot{\mathbf{x}}(t) = \mathbf{A}\mathbf{x}(t) + \mathbf{h}(\mathbf{x}) + \mathbf{B}\mathbf{u}(t) \tag{11}$$

where $\mathbf{x} \in \mathbb{R}^n$ is the state vector, $\mathbf{u} \in \mathbb{R}^m$ is the control inputs, $\mathbf{A} \in \mathbb{R}^{n\times n}$ and $\mathbf{B} \in \mathbb{R}^{n\times m}$ are constant real matrices, and $\mathbf{h}(\mathbf{x}) \in \mathbb{R}^n$ is a vector whose elements are nonlinear functions of $\mathbf{x}$.

3.1 Rotational State-Space Model

The rotational MAV state-space model is given by

$$\mathbf{x} \triangleq \begin{bmatrix} \phi & \theta & \psi & \Omega_x & \Omega_y & \Omega_z \end{bmatrix}^{\mathrm{T}} \in \mathbb{R}^6, \tag{12}$$

$$\mathbf{u} \triangleq \mathbf{T}^c \in \mathbb{R}^3, \tag{13}$$

and

$$\mathbf{A} = \begin{bmatrix} 0&0&0&1&0&0 \\ 0&0&0&0&1&0 \\ 0&0&0&0&0&1 \\ 0&0&0&0&0&0 \\ 0&0&0&0&0&0 \\ 0&0&0&0&0&0 \end{bmatrix} \tag{14}$$

Table 1. Parameters of AR Drone 2.

Variables	Values	Unit
Mass of AR Drone 2, m	0.429	kg
Acceleration of gravity, g	9.80665	m/s^2
Arm lenght, l	0.1785	m
Moment of inertia for x-axis, J_x	2.238×10^{-3}	kg.m^2
Moment of inertia for y-axis, J_y	2.986×10^{-3}	kg.m^2
Moment of inertia for z-axis, J_z	4.804×10^{-3}	kg.m^2
Moment of inertia of each rotor, I_r	2.030×10^{-5}	kg.m^2
Force coefficient k_f	8.050×10^{-6}	N/(rad/s)^2
Torque coefficient, k_τ	2.423×10^{-7}	N.m/(rad/s)^2
Time constant, τ	4.718×10^{-3}	s
Maximum speed of the motor, $\omega_{\max}$	1047	rad/s

$$\mathbf{B} = \begin{bmatrix} 0 & 0 & 0 \\ 0 & 0 & 0 \\ 0 & 0 & 0 \\ \frac{1}{J_x} & 0 & 0 \\ 0 & \frac{1}{J_y} & 0 \\ 0 & 0 & \frac{1}{J_z} \end{bmatrix} \tag{15}$$

$$\mathbf{h}(\mathbf{x}) = \begin{bmatrix} \frac{1}{2}(-\psi^2\Omega_x + \theta^2\Omega_x) - \phi\Omega_y \\ \psi\Omega_x - \frac{\psi^2\Omega_y}{2} \\ -\theta\Omega_x + \psi\theta\Omega_y \\ \frac{(J_y - J_z)}{J_x}\Omega_y\Omega_z - \frac{I_r\Omega_y}{J_x}(\omega_1 - \omega_2 + \omega_3 - \omega_4) \\ \frac{(J_z - J_x)}{J_y}\Omega_x\Omega_z + \frac{I_r\Omega_x}{J_y}(\omega_1 - \omega_2 + \omega_3 - \omega_4) \\ \frac{(J_x - J_y)}{J_z}\Omega_x\Omega_y \end{bmatrix} \tag{16}$$

4 Control Design

In this section, we present a control strategy to drive the MAV's nonlinear dynamics from a certain initial condition to a desired state. Following the control method proposed by [5], we formulate an optimal control problem that, given the nonlinear dynamics in Eq. (11), aims at minimizing the following LQR-like cost function:

$$J = \int_0^\infty (l(\mathbf{x}) + \mathbf{u}^T\mathbf{R}\mathbf{u})dt \tag{17}$$

where $\mathbf{R} \in \mathbb{R}^{m\times m}$ is a positive definite matrix and $l(\mathbf{x}) \in \mathbb{R}$ is a function related to the weights of the dynamical states over time. Function $l(\mathbf{x})$ will be selected as follows to account for the nonlinear terms in the dynamical model.

Propostion: Let $l(\mathbf{x})$ be

$$l(\mathbf{x}) = \mathbf{x}^T\mathbf{Q}\mathbf{x} - \mathbf{h}(\mathbf{x})^T\mathbf{P}\mathbf{x} - \mathbf{x}^T\mathbf{P}\mathbf{h}(\mathbf{x}) \tag{18}$$

where $\mathbf{Q} \in \mathbb{R}^{n\times n}$ and $\mathbf{P} \in \mathbb{R}^{n\times n}$ are real symmetric positive definite matrices and $\mathbf{P}$ is the solution of the matrix algebraic Riccati equation

$$\mathbf{P}\mathbf{A} + \mathbf{A}^T\mathbf{P} - \mathbf{P}\mathbf{B}\mathbf{R}^{-1}\mathbf{B}^T\mathbf{P} + \mathbf{Q} = 0. \tag{19}$$

Then, as long as $l(\mathbf{x})$ is positive definite, the linear feedback control law

$$\mathbf{u} = -\mathbf{R}^{-1}\mathbf{B}^T\mathbf{P}\mathbf{x} \tag{20}$$

is optimal in order to transfer the nonlinear system in Eq. (2) from an initial condition $\mathbf{x}(0)$ to the origin while minimizing the cost function in Eq (3). Additionally, the controlled system is locally asymptotically stable in the neighborhood $\Gamma_0 \subset \Gamma, \Gamma \subset \mathbb{R}^n$, of the origin if $\mathbf{x}(0) \in \Gamma_0$. If $\Gamma = \mathbb{R}^n$, then the controlled system is globally asymptotically stable.

Proof: See Rafikov and Balthazar [5].

5 Simulation Tests

The simulation uses three-degree-of-freedom nonlinear equations of the attitude of the MAV and are implemented in Matlab/Simulink. In this section, numerical simulations are presented to verify the effectiveness of the proposed method. In these numerical simulations, the initial condition $\mathbf{x}(0)$ is given by

$$\mathbf{x}(0) = [30\ 20\ 10\ 0\ 0\ 0]^{\mathrm{T}}. \tag{21}$$

Choose

$$\mathbf{Q} = \begin{bmatrix} 17 & 0 & 0 & 0 & 0 & 0 \\ 0 & 17 & 0 & 0 & 0 & 0 \\ 0 & 0 & 17 & 0 & 0 & 0 \\ 0 & 0 & 0 & 1 & 0 & 0 \\ 0 & 0 & 0 & 0 & 1 & 0 \\ 0 & 0 & 0 & 0 & 0 & 1 \end{bmatrix} \tag{22}$$

and

$$\mathbf{R} = \begin{bmatrix} 1 & 0 & 0 \\ 0 & 1 & 0 \\ 0 & 0 & 1 \end{bmatrix} \tag{23}$$

we obtain

$$\mathbf{P} = \begin{bmatrix} 4.16 & 0 & 0 & 0.01 & 0 & 0 \\ 0 & 4.17 & 0 & 0 & 0.01 & 0 \\ 0 & 0 & 4.20 & 0 & 0 & 0.02 \\ 0.01 & 0 & 0 & 0.002 & 0 & 0 \\ 0 & 0.01 & 0 & 0 & 0.003 & 0 \\ 0 & 0 & 0.02 & 0 & 0 & 0.01 \end{bmatrix} \tag{24}$$

by solving the Riccati Eq. (19). Then, from Eq. (20) one obtains

$$\mathbf{u} = \begin{bmatrix} 4.123 & 0 & 0 & 1.01 & 0 & 0 \\ 0 & 4.123 & 0 & 0 & 1.012 & 0 \\ 0 & 0 & 4.12 & 0 & 0 & 1.02 \end{bmatrix} \mathbf{x} \qquad (25)$$

The behavior of the attitude angles can be seen in Figure 2. The simulations show that the function $l(\mathbf{x})$ calcu-

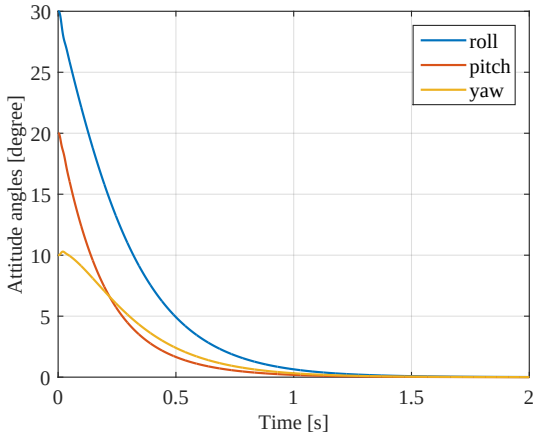

Fig. 2. Euler angles over time.

lated for the attitude dynamics of the MAV is positive, as illustrated in Figure 3, which guarantees asymptotic stability according to Rafikov and Balthazar's theorem.

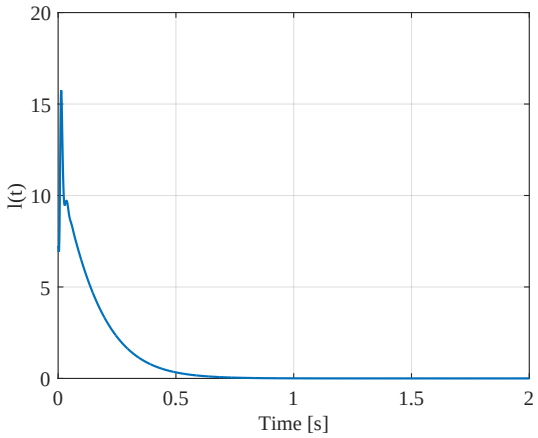

Fig. 3. Positive function $l(t)$, calculated for the attitude dynamics of the MAV.

The control signals, presented in Figure 4, lie within the acceptable range for a real MAV, i.e. ±2.28 N.m.

6 Conclusion

This paper have presented the attitude control of a MAV by designing the linear feedback controller. The linear feedback control problem was formulated under the optimal control theory viewpoint. Asymptotic stability of the closed-loop nonlinear system is guaranteed by means of a Lyapunov function as presented in [5].

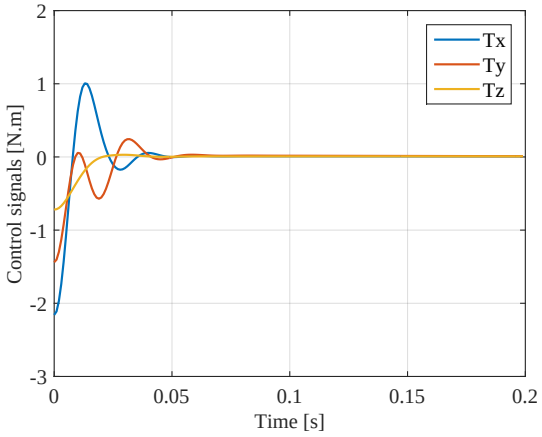

Fig. 4. Control signals over time.

7 Acknowledgments

The authors thank Coordenação de Aperfeiçoamento de Pessoal de Nível Superior (CAPES) and Conselho Nacional de Desenvolvimento Científico e Tecnológico (CNPq) for financial supports.

References

1. S. Bouabdallah, A. Noth, and R. Siegwart. Pid vs lq control techniques applied to an indoor micro quadrotor. In *Proceedings of the IEEE/RSJ International Conference on Intelligent Robots and Systems*, pages 2451–2456, New Orleans, September 2004.
2. S. Bouabdallah and R. Siegwart. Backstepping and sliding-mode techniques applied to an indoor micro quadrotor. In *Proceedings of the IEEE International Conference on Robotics and Automation*, pages 2247–2252, Barcelona, April 2005.
3. T. Cheviron, T. Hamel, R. Mahony, and G. Baldwin. Robust nonlinear fusion of inertial and visual data for position, velocity and attitude estimation of uav. In *Proceedings of the IEEE International Conference on Robotics and Automation*, pages 2010–2016, Roma, April 2007.
4. G. V. Raffo, M. G. Ortega, and F. R. Rubio. An integral predictive/nonlinear $\mathcal{H}_\infty$ control structure for a quadrotor helicopter. *Automatica*, 46(1):29–39, 2010.
5. M. Rafikov and J. M. Balthazar. On control and synchronization in chaotic and hyperchaotic systems via linear feedback control. *Communications in Nonlinear Science and Numerical Simulation*, 13(4):1246–1255, 2008.
6. D. A. Santos, O. Saotome, and A. Cela. Trajectory control of multirotor helicopters with thrust vector constraints. In *21st Mediterranean Conference on Control and Automation*, pages 375–379, Chania, 2013.
7. S. Saripalli, J. F. Montgomery, and G. S. Sukhatme. Visually-guided landing of an unmanned aerial vehicle. *IEEE Transactions on Robotics and Automation*, 10(3):371–381, 2003.